

RESEARCH ARTICLE

Drought Detection in Satellite Imagery: A Layered Ensemble Machine Learning Approach

Muhammad Owais Raza¹ · Naeem Ahmed Mahoto² · Mana Saleh Al Reshan^{3,4} · Ali Alqazzaz⁵ · Adel Rajab⁶ · Asadullah Shaikh^{3,4}

Received: 10 February 2025 / Revised: 13 May 2025 / Accepted: 20 June 2025
© The Author(s) 2025

Abstract

Drought has been a major calamity due to climate change in recent years. Predicting drought has grabbed the attention of meteorologists and climate scientists, who study and look for modern techniques. The early detection of drought leads to better management of resources and timely decisions to avoid damage. Machine learning techniques have proven their potential in classification and prediction problems. This study proposes a layered ensemble machine learning approach to detect drought from satellite imagery. The satellite imagery is collected using Google Earth Pro for the region 'Tharparkar' in Pakistan's Sindh province. Tharparkar is one of the most drought-stricken regions in Pakistan. The proposed approach combines conventional machine learning algorithms (Support Vector Machine (SVM), Logistic Regression (LR), Decision Tree (DT), Random Forest (RF), Naive Bayes (NB), and k-Nearest Neighbor (k-NN)) with ensemble methods (Bagging and Voting) in a layered fashion for detecting drought from satellite imagery. The novelty of the study lies in its layered ensemble architecture that integrates multiple conventional classifiers with ensemble techniques for improved drought detection accuracy using satellite imagery. The validation of the model is computed using the stratified split method. The developed classification model is evaluated using well-established indexes, including accuracy, precision, recall, F measure, and Area Under Curve (AUC). Among the classical models, the Decision Tree classifier performed best with an accuracy of 82.17%, a precision of 82.53%, a recall of 82.28%, and an F1 score of 82.35%. Within the Bagging models, Bagged Decision Tree achieved the highest performance, attaining an accuracy of 84.78%, a precision of 85.14%, a recall of 84.87%, and an F1 score of 84.91%. The final-layer Voting ensemble outperformed all previous models, yielding the highest F1 score of 84.80%. Based on experimental results, the proposed model has strong potential for practical deployment in real-world environmental monitoring systems.

Keywords Machine learning · Remote sensing · Satellite imagery · Ensemble learning · Image classification

Abbreviation

| | |
|------|---|
| SVM | Support vector machine |
| LR | Logistic regression |
| M | Machine learning |
| DT | Decision tree |
| R | Random forest |
| NB | Naive Bayes |
| KNN | K-Nearest neighbor |
| AUC | Area under curve |
| SPI | Standardized precipitation index |
| SPEI | Standardized precipitation evapotranspiration index |



WFL Wavelet-fuzzy logic
HSMDI High-resolution soil moisture drought index

1 Introduction

Drought remains one of the most severe risks, wreaking havoc on the environment, society, and economy on a large scale. Droughts in large portions of Central Europe in the summer of 2018 resulted in major wildfires and crop failures. Only in Germany was the damage projected to be in the hundreds of millions of euros [1]. Besides, global warming directly impacts the frequency and the intensity of extreme occurrences such as droughts due to huge changes in the Earth's climate system [2]. An increase in the frequency of drought occurrences poses a significant threat to coming generations. Therefore, comprehensive knowledge of the drought phenomena is required to intervene early and prevent drought disasters. A drought prediction system would allow stakeholders to mitigate the risks associated with drought occurrences. It may also help in resource management and timely decision-making strategies to cope with extreme conditions of water shortage, hunger, and starvation.

Machine Learning has proven its significance and usefulness in predictive analysis, which is near to impossible manually. The applications of machine learning, apart from structured textual data, also include Image processing, computer vision, and object detection and recognition. Satellite imagery research is one of the key areas in machine learning, which may help in detecting drought regions. Drought prediction is of difficult and challenging task which requires sophisticated and automated methods.

The drought data is computed through the Standardized Precipitation Index (SPI), and Standardized Precipitation Evapotranspiration Index (SPEI) which are multiscalar drought indexes based on climate data. Another source of drought data can be meteorological factors, such as wind, temperature, humidity, and many more. These features are also used in the predictive analysis of droughts. Traditional meteorological drought indices, such as SPI and PDSI, depend on long-term precipitation or climatic data and often face delays in detection, and on the other hand, real-time satellite images offer faster and more spatially granular drought identification.

A layered ensemble machine learning approach is proposed to predict drought-hit spots of Tharparkar, located in the Sindh Province of Pakistan. A custom-made dataset using Google Earth Pro was built for the experiments, which comprised satellite images of Tharparkar.

The key contributions of the study are reported in the following:

1. A layered ensemble machine learning approach is proposed for detecting drought from satellite imagery.
2. A custom-made dataset creation from satellite imagery of Tharparkar region.
3. The comparison of the proposed layered approach with conventional machine learning for drought predictive analysis.

The rest of this paper is organized as Sect. 2 reports a literature review on drought prediction. Section 3 is Material and Methods that discusses the proposed layered ensemble machine learning approach. Section 4 presents the experimental evaluation of the study and Sect. 5 draws conclusions.

2 Literature Review

Drought is one of the world's most challenging and devastating natural calamities. Droughts generally result in considerable loss of human life and resources. Therefore, it's critical to keep an eye on them on a frequent basis. Droughts have become more widespread in recent years in many places of the world. Considering the droughts in East Africa in 2010–2011, Texas in 2012, the United States Central Great Plains in 2012, and California in from 2012 to 2015 [3].

These repercussions are far more severe in Pakistan, which is one of the worst drought-affected countries due to its substantial reliance on agriculture. Nearly 43% of Pakistan's workforce is employed in agriculture [4], which makes drought prediction and forecasting one of the key challenges for Machine Learning and Artificial Intelligence. Various researchers have used machine learning for this purpose as in [5], SVM and group data processing methods were used to discover correlations, which were then used to forecast the drought using SPI. Researchers in [45] developed cubist model for improved soil moisture estimation in Gansu for drought prediction, reducing RMSE and MAPE by 26% and 28%. [45] shows environmental factors, especially DEM, lowered RMSE by 25%, while meteorological factors contributed 6.5%. SPI has been used in combination with SPEI to forecast drought indexes. They evaluated by comparing ARIMA and LSTM and came to the conclusion that Arima is much more reliable and highly inexpensive than LSTM. Researchers developed an ML system designed to detect and forecast drought utilizing data from Landsat vegetation indices in [11]. [7] developed a machine learning stacking ensemble to predict 3-month SPEI in China using PERSIANN-CDR, MODIS, and climate zoning data. CatBoost Regressor (CBR) performed best, achieving $R^2 = 0.9065$ (east) and 0.8218 (west). [8] study uses machine learning to forecast drought in semi-arid India using SPI for 3 and 6 month periods. Based on data from 1989 to 2019, the Matern Gaussian Process Regression model achieved the highest determination coefficient ($R^2 = 0.95$ for SPI-3 and 0.93 for SPI-6). [9] compares four machine learning models RF, CNN, SVR, and BP for drought monitoring in Inner Mongolia. The RF model performed best, with an R^2 of 0.44–0.79 and RMSE of 0.44–0.72. The models were tested on data from June to September, with RF showing the highest correlation with SPEI (0.78) compared to CNN (0.79), SVR, and BP.

The different sources and techniques used for the satellite remote sensing data are reported in Table 1. In [37], the Standardized Precipitation Evapotranspiration Index (SPEI) and machine learning have been combined to analyze drought in the Tibetan Plateau, for instance, using CNN, RF, XGB, and LSTM techniques. Another study [38] employed lagged SSI values to predict extended droughts in the Gunnison River Basin using a Deep Belief Network (DBN). [39] showed how multi-source remote sensing data can enhance drought forecasting by integrating satellite data from MODIS and TRMM into a deep learning model in Henan Province, China. Furthermore, ANN and stochastic methods have been combined in hybrid models to forecast drought conditions in India [41], while Long Short-Term Memory (LSTM) models have been used to predict drought based on rainfall data in Iran [40]. The use of adaptive neural fuzzy inference systems (ANFIS) for forecasting drought in central Anatolia, Turkey, has been studied in [42], and SVM for forecasting seasonal variations in SPI in the Tehran reservoir basins is shown in [13]. Furthermore, in [23], in New South Wales, Australia, models, such as RF, SVM, and MLP, demonstrated high prediction accuracy when drought variables based on remote sensing such as SPI were used. The integration of wavelet transform analysis with machine learning algorithms, such as SVR and ANN, was found to improve drought prediction based on vegetation indices and land cover [24]. These studies collectively emphasize the growing role of machine learning techniques, especially when combined with satellite and remote sensing data, in improving drought forecast accuracy and decision-making.

To achieve the best results, researchers used a variety of machine learning methods, such as (MLPNN) multilayer perceptron neural network and (MLR) multiple linear regression, a, and a (CANFIS) coactive neuro-fuzzy inference system in [12]. In this study [13], a very well-known machine learning technique known as SVM is used to anticipate seasonal variations in the SPI in four reservoir watersheds that supply water to Tehran, Iran's capital city [13]. Wavelet transformations, for example, were used in combination with ML methods to enhance predictive performance [14] All these techniques were applied on one or more than one index which was obtained using remote sensing. There could be other indicators as well such as in [15], researchers have used soil moisture as an indicator and created High-Resolution Soil Moisture Drought Index (HSMDI) and used Random forest to predict drought. When drought comes, visual differences in scenery, greenery vanishes and grass-covered land can be seen. All these features are visible from satellite imagery as in [16] various stages of drought are classified using machine learning. [16] lays a preliminary path for this research.

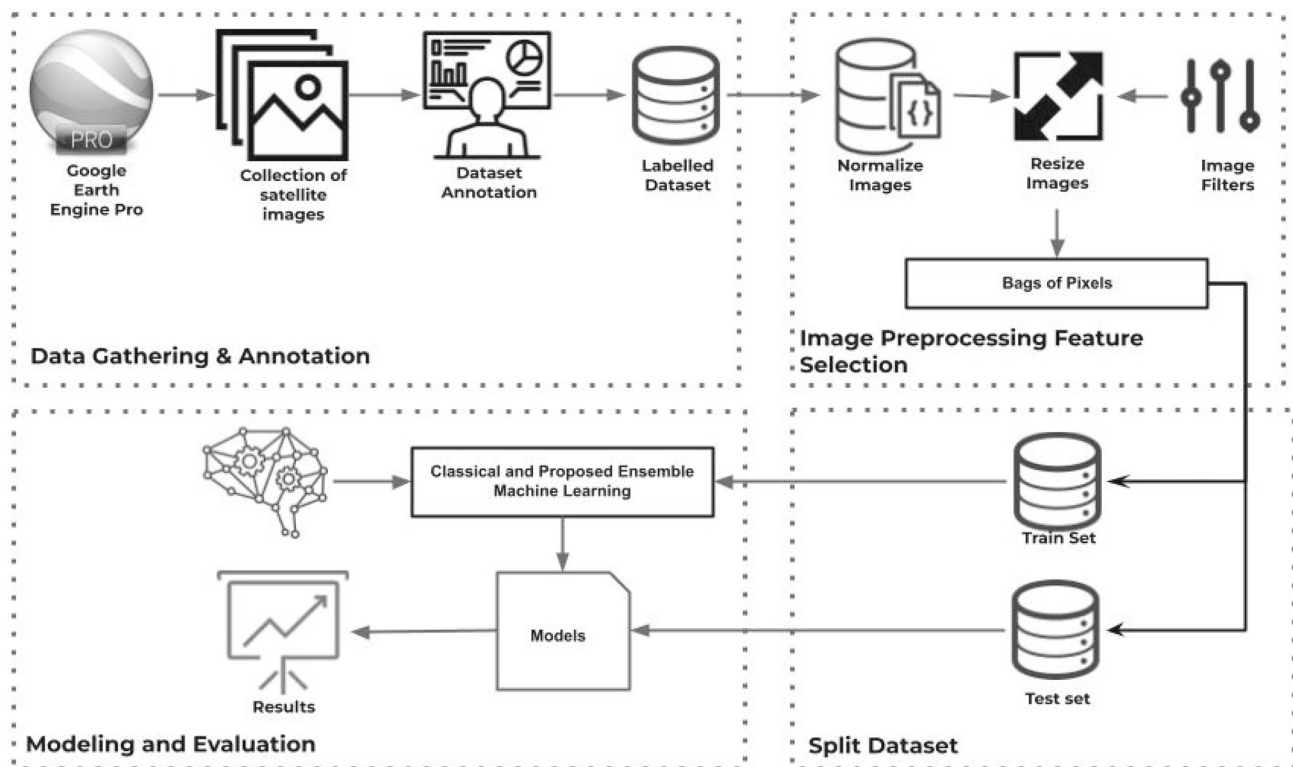


Fig. 1 Building Blocks of Research Methodology

In this study, we are not using any remote sensing index or any specific drought index to predict drought but rather raw satellite images are used. A layered Ensemble approach is used to perform prediction of whether an image is showing drought or normal conditions.

3 Materials and Methods

Figure 1 represents the research method employed in this study.

There are 4 parts of this research method: (1) Data Collection and Annotation, (2) Image Pre-processing and Feature Selection, (3) Split Dataset, and (4) Modeling and Evaluation. The details of each part are explained in the following:

3.1 Data Collection and Annotation

The unavailability of satellite images benchmark dataset for the drought and normal conditions of Tharparkar region located in Sindh Province of Pakistan led to the collection of the required dataset. Therefore, Satellite images have been captured using Google Earth Pro with help of historical image features for the different timings of the region. Tharparkar region is the most drought-affected region in Pakistan. The population of Tharparkar is 1.65 million in 2021. There are seven talukas in Tharparkar. Anthropogenic changes such as deforestation or urban expansion are rare in this area, so vegetation loss due to factors not related to drought, such as deforestation or urbanization, is not often observed. Data collection was conducted across all seven talukas of the Tharparkar district to ensure comprehensive geographic coverage and representation of the region's diverse environmental conditions. Figure 2 illustrates the Tharparkar district, clearly highlighting the individual talukas involved in the study.

Table 1 Literature review for the source of data and techniques for drought modeling

| Paper | Description | Data | Technique |
|-------|---|---|--------------------------|
| [37] | A Fusion of machine learning and (SPEI) is proposed in this study for drought analysis in a reflective case analysis throughout the Tibetan Plateau in China from 1980 to 2019 | SPEI | SPEI, CNN, RF, XGB, LSTM |
| [38] | Using deep learning algorithms, this study investigates the drought prediction problem. Researchers propose a DBN for protracted drought prediction utilizing lagged SSI values as inputs. The proposed model is used to forecast various time scale indicators throughout the Gunnison River Basin | SSI | DBN |
| [39] | The diverse hazard variables in drought development were thoroughly considered using satellite data from MODIS and TRMM as multi-source remote sensing information. A deep learning model was tested in Henan Province, China | MODIS, TRMM | DNN |
| [40] | This study investigates the potential of a DL method to forecast drought using monthly rainfall data from four Iranian stations | Rainfall data | LSTM |
| [41] | The hybrid approach combines the benefits of ANN and stochastic models. The hybrid model, in addition to individual ANN and stochastic models, was used to forecast droughts throughout the Kansabati River in India using the SPI series | SPI | ANN |
| [13] | A well-known machine learning technique SVM is employed to predict seasonal fluctuations in SPI in 4 reservoir basins supplying Tehran, Iran's capital | SPI | ANN, SVM |
| [42] | The applicability of the ANFIS for drought forecasting and the numerical value of drought indices, such as SPI, are investigated. Ten rainfall gauging stations in Central Anatolia, Turkey, were chosen as the study area | SPI | ANFIS, FFNN |
| [43] | Various ANN and ANFIS models were used with meteorological variables like precipitation, temperature, wind speed, and evaporation | Wind, Temperature, Precipitation, Evaporation | ANN, ANFIS, TLRN |
| [23] | Thirty remote sensing-based drought variables from TTRMM and MODIS satellite sensors were used to replicate a drought indicator, SPEI, for New South Wales, Australia | SPEI | RF, SVM, MLP |

Table 1 continued

| Paper | Description | Data | Technique |
|-------|--|---|---|
| [24] | Wavelet-transform-analysis combined with SVR and ANN for drought prediction using vegetation indices, land cover, and surface discharge | SPI, NDVI, NDWI | SVR, ANN, Wavelet-Transform |
| [25] | An ANN model for drought conditions prediction using satellite imagery and standardized SPI | NDVI, VCI, TCI, SPI, Satellite imagery | SVM, ANN |
| [26] | Monitoring drought in South Africa using DL approach and remote sensing data, incorporating precipitation, soil, and vegetation data | VCI, TCI, VHI, SMDI, EDI, PAI, PCI, SPI, SPEI | DFNN |
| [27] | Developed drought prediction ML models over Pakistan utilizing SVM, ANN, and KNN, classifying droughts into moderate, severe, and extreme categories | SPEI | SVM, ANN, KNN |
| [28] | Investigated ANN and SVR for drought forecasting over different lead times with hybrid transformation techniques | SPI | ANN, SVR |
| [29] | Created a drought vulnerability map (DVM) using novel ensemble ML algorithms | Rainfall | PSO, RF, PSO-RF, MLP, PSO-MLP, SVR, Bagging |
| [16] | Drought prediction using satellite imagery over a drought-prone region in Pakistan with classical and ensemble ML techniques | Satellite imagery | Bagging, Boosting, Ensemble |
| [30] | Developed an integrated model for improving satellite precipitation data for drought analysis in Central India | SPI | RF |
| [31] | Examined climate fascicles related to droughts and used them to generate an ensemble drought predictive model over Western Rajasthan using SVM | SPI | SVM |
| [32] | Drought forecasting using enhanced vegetation index with ML techniques and comparing results with MODIS products | EVI | Gradient Boosting |
| [33] | Developed a novel drought index (CTEI) modeled using five ML techniques | CTEI | SVM, DT, Boosted DT, Bagged DT, Gaussian Regression |
| [34] | Evaluated the potential hazard of reduction in yield under drought using CMIP6 climate models | SPEI | RF, GBM |
| [36] | Developed a wavelet-fuzzy logic (WFL) fusion model for long-term drought forecasting | SPTI | Fuzzy Logic |
| [35] | Drought forecasting using an ANN model to predict numerical dryness indicators from rainfall data | EDI, SPI | ANN |



Fig. 3 Sample of collected and annotated dataset

Table 2 Comparison between traditional and proposed image-based drought detection approaches

| Aspect | Traditional Methods (SPI/SPEI + Remote sensing) | Proposed image-based approach |
|---------------|--|--|
| Data Type | Meteorological + satellite indices (e.g., SPI, SPEI) | Raw satellite images (pixel-based features) |
| Granularity | Continuous severity scales | Binary/Categorical classification |
| Timeliness | May involve delay due to historical data dependency | Real-time detection using current satellite imagery |
| Complexity | Requires data preprocessing, index computation | Simpler pipeline using direct image classification |
| Applicability | Best for detailed monitoring and risk analysis | Effective for early alerts and image-rich, data-sparse regions |
| Robustness | Affected by gaps in weather station data | Works well if imagery is consistently available |

The collected satellite images dataset was annotated into two classes: *drought* and *no-drought*. Each image is composed of a timestamp. Thus, annotation is carried out as *drought* if the timestamp is of the time when there was a drought in the region. Likewise, *no drought* is labeled when there was no drought in the region according to the image timestamp. The temporal resolution was variable, with images chosen to represent different time periods and labeled according to their timestamps matched with official drought data [45]. During annotation, the alignment between the recorded timestamp of the the collected images and drought records [45] was strictly observed. Usually, drought is observed in the region during the summer season of the year and no-drought during the winter and spring seasons of the year. The collected and annotated dataset contains a total of 600 images, with 300 images each for drought and normal conditions, resulting in a balanced dataset. A sample of the collected and annotated dataset is shown in Fig. 3.

The Table 2 highlights key differences between traditional drought detection methods relying on indices, such as SPI, SPEI, NDVI, and our proposed image-based approach. While traditional methods offer continuous severity scales, they often require multisource data and preprocessing. In contrast, our method provides a simpler pipeline using raw satellite images, which offers timely predictions that are especially useful in data scarce regions.

3.2 Image Pre-processing and Feature Selection

Pre-processing is applied to the collected and annotated dataset in order to make it consistent, which is one of the most important elements for better results. The pre-processing normalized and reduced the size of an image to 200×200 pixels. Image enhancement technique i.e., an image sharpening filter, was also applied for clear visibility

and further processing. The experiments showed better results with a 5×5 sharpening filter. The processed dataset contains sharpened 200×200 images of 3×3 dimensions i.e., RGB (color image).

A pixel of an image is considered a feature [44] and a feature vector is created for an image. The created feature vector is used for training and testing purposes in the prediction analysis. In this study, feature selection was done using the Bag of Pixels method. In this method, each satellite image was transformed into a flattened vector of raw pixel intensities. This method allows the model to learn directly from the raw pixel distributions across the dataset, capturing texture and spatial patterns without the need for handcrafted features. As the study makes use of classical and ensemble machine learning algorithms, this method provided the simplest and most computationally effective means of feature extraction.

3.3 Dataset Split

Predictive analysis requires two datasets. One for the training and another for the testing. The processed dataset was divided into two subsets. Both subsets contain a disjoint set of images. The training subset trains the model for the prediction and the test subset evaluates the performance of the predictive model. The splitting technique, used in this study, is stratified split as it is one of the most common splitting approaches as evident from the literature. The 80–20% split is widely considered an optimal choice for training and evaluating machine learning models, especially when working with moderately sized datasets, as it strikes a balance between having sufficient training data to learn from and adequate test data to assess generalization performance. This splitting ratio is particularly effective for datasets with limited size, like in this study, where maximizing learning while retaining reliable evaluation is essential. Hence, an 80–20% splitting ratio [10] is adopted in the experiments of this study, where 80% of the data is used for training and 20% for testing.

3.4 Modeling and Evaluation

In order to perform data modeling, classical and ensemble machine learning approaches are applied for the experiments. Classical machine learning algorithms include Support Vector Machine, Logistic Regression, Decision Tree, Random Forest, Naive Bayes, and k-Nearest Neighbor. Bagging and Voting are applied as ensemble methods. A novel ensembling architecture is proposed to detect drought in satellite images. Despite the smaller size of the dataset, the proposed strategy performs well for drought detection and prediction. Lets discuss the proposed approach in detail.

3.4.1 Proposed Layered Ensemble Approach

The layered Ensemble approach proposed in this paper is shown in Fig. 4. There are three layers in this technique: (1) the classical layer, (2) the Bagging layer and (3) the Voting layer. In the first layer, classical machine learning approach is applied, bagging in the second layer, and voting is applied in the third layer to find out the most suitable model. The details of each layer are reported as follows:

The classical layer contains six conventional machine learning algorithms into account, namely Support Vector Machine (SVM), Logistic Regression (LR), Decision Tree (DT), Random Forest (RF), Naive Bayes (NB) and K Nearest Neighbor (KNN). The algorithms were chosen because Support Vector Machine (SVM), Logistic Regression (LR), and Naive Bayes (NB) offer robust baselines known for their simplicity and interpretability. Decision Tree (DT) and k-Nearest Neighbor (k-NN) capture complex decision boundaries, while ensemble methods like Random Forest (RF) leverage multiple weak learners to improve accuracy and reduce overfitting. Each algorithm is represented as C_i , where i ranges from 1 to 6. The order of these models is based on their performance. C_1 represents the best-performing model, C_2 is the second-best model, and C_6 is the least accurate one. The purpose of this layer is to create classical machine learning models to be used for further processes in the prediction analysis. Details of each conventional methods are discussed as follows:

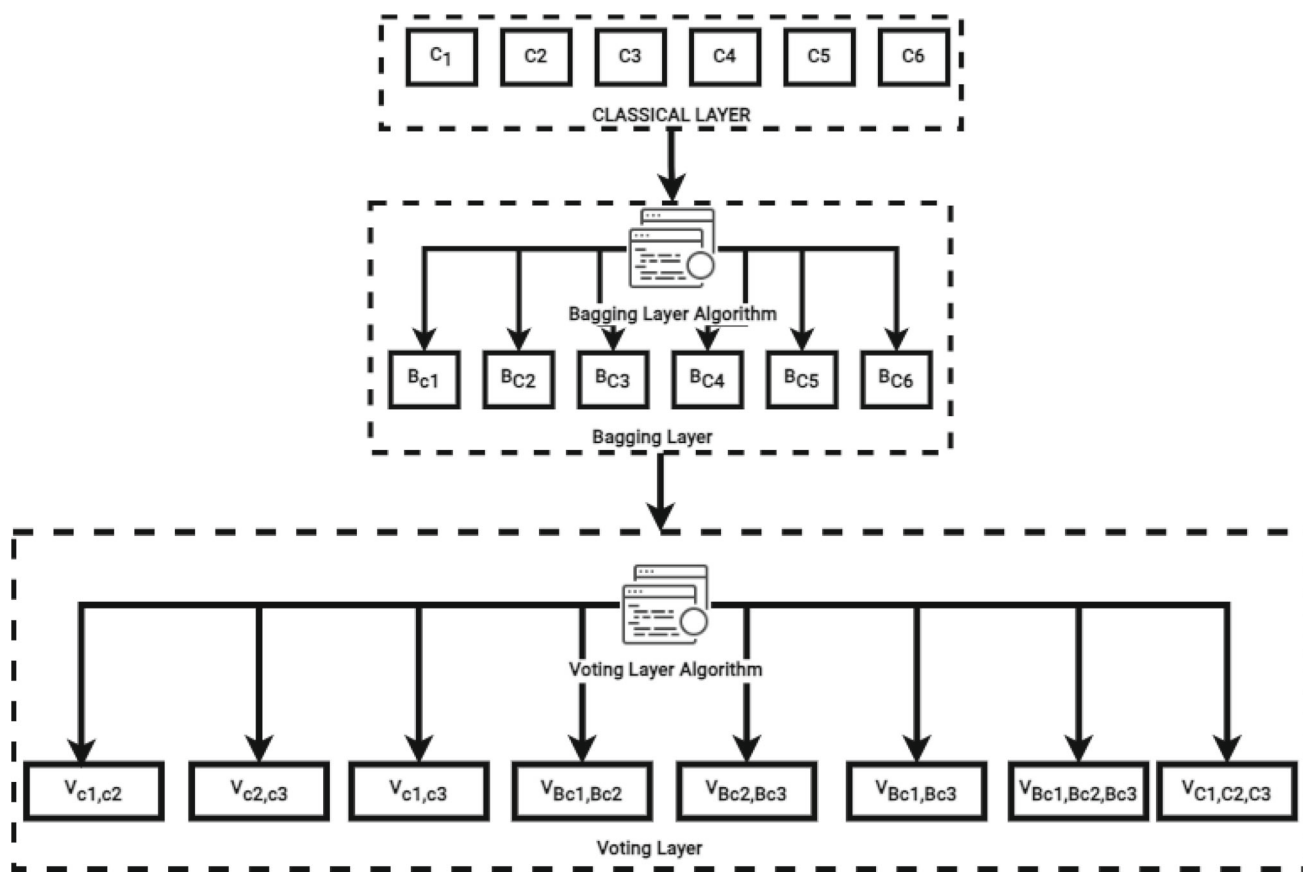


Fig. 4 Proposed layered ensemble approach

Support vector machine (SVM) is a supervised learning model for regression analysis and classification that evaluates data and identifies patterns. SVM differentiates examples with distinct class labels by building hyper-planes in a multidimensional space. SVM, being continuous in nature, can handle many categorical variables and can perform regression as well as classification tasks. Figure 5 shows the function of SVM. SVM is useful for the high domains, even though the dimensionality and number of samples increase. It has a lot of memory and is quite adaptable. If the feature size is substantially more than the amount of data, then it is likely to perform poorly. This is the reason that the features of the considered dataset are really high compared to the amount of data. Thus, SVM is expected to perform well [17].

The sigmoid function is used to transform a linear regression into Logistic Regression (LR). The likelihood for a specific categorization is represented by the vertical axis, while the value of x is represented by the horizontal axis. It is assumed that the $X|Y$ distribution is of the Bernoulli type. The following is the Logistic Regression formula represented in Eq. 1.

$$F(x) = \frac{1}{1 + e^{\beta_0 + \beta_1 x}} \tag{1}$$

where $\beta_0 + \beta_1 x$ is similar to $y = c + mx$

The logistic function uses a sigmoid activation function to limit the y value of a large scale to a range of 0–1. These values are used for classification. if the value is less or equal to 0.5, it will be assigned 0 class; or if it is greater than 1, then it will be the assigned class [18].

A decision Tree (DT) is a general-purpose machine learning algorithm that can be used in a wide range of situations. It is one of the most useful methods of supervised learning. DT is a tree-like network in which nodes

Fig. 5 SVM working functionality diagram

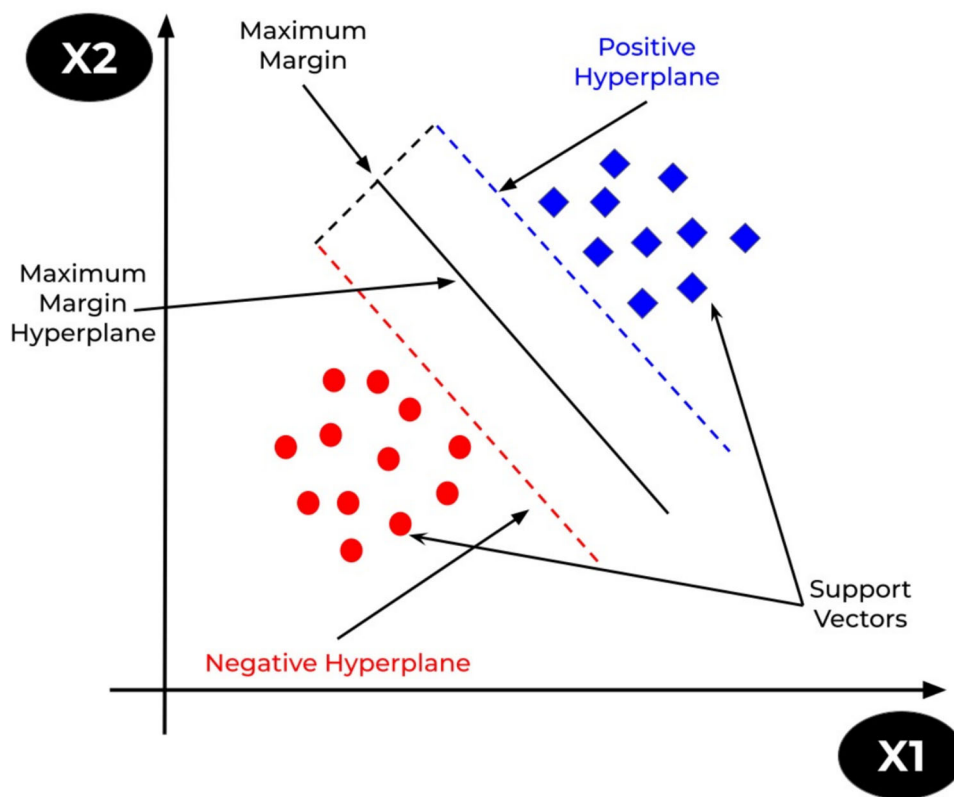
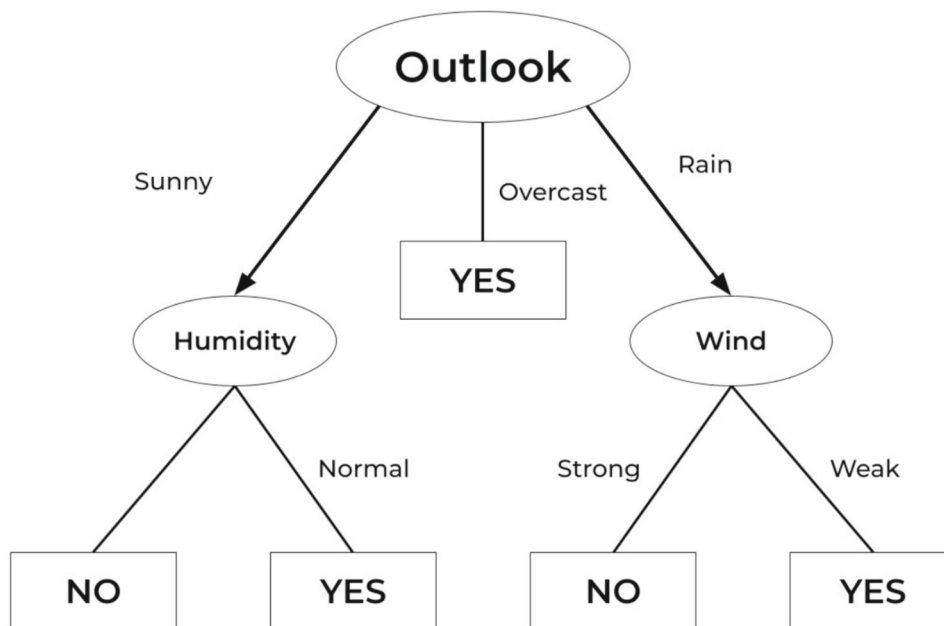


Fig. 6 Decision working Process diagram



indicate the instances, where a feature is chosen and a question is posed; the edge represents the responses to the question; and the leaves of the tree represent the real class label. DT is used in the nonlinear decision-making process [19]. The main reason for selecting this algorithm for this study is its simplicity. Figure 6 shows the example of a Decision Tree.

Random Forest (RF) is a machine learning (ML) model that uses the results of a series of decision trees to predict the output. Each tree is built independently and is based on a random vector selected from the data input,

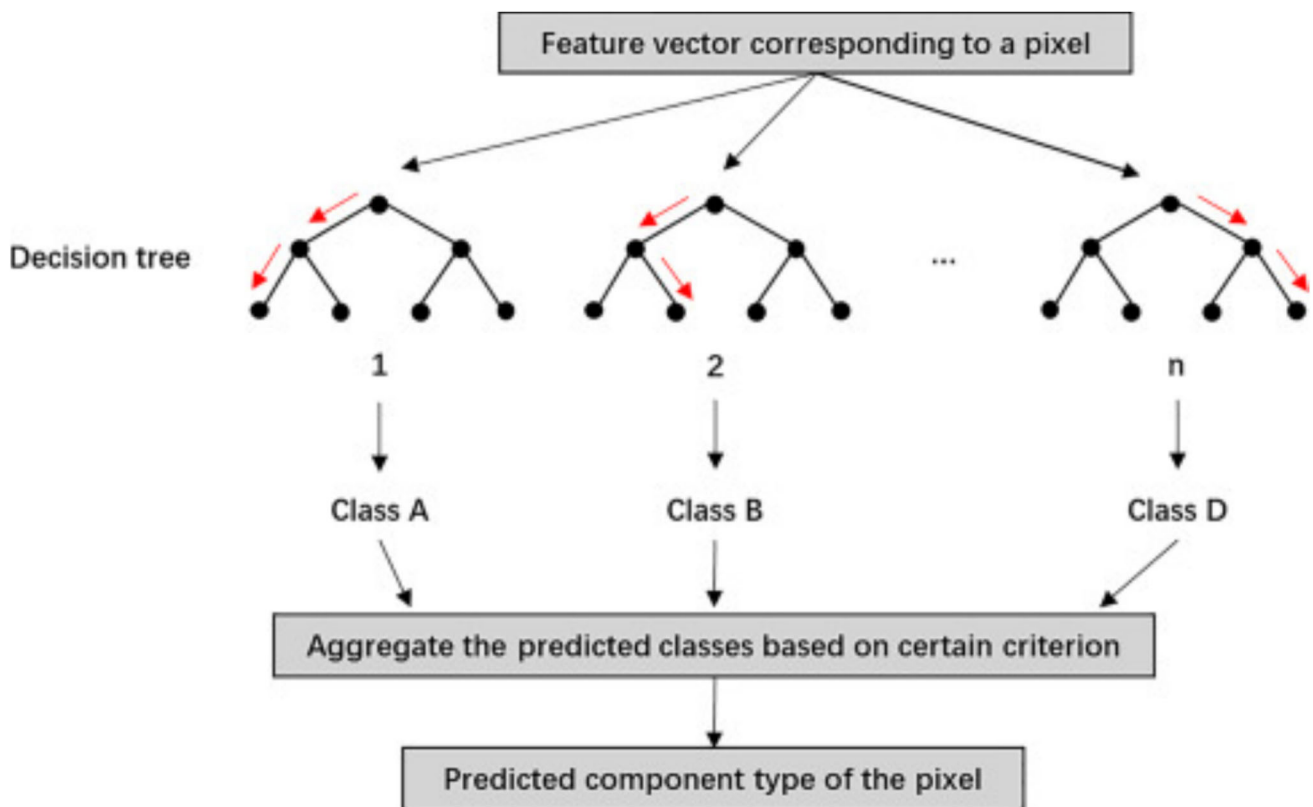


Fig. 7 Random forest working process diagram

with the same distribution across the forest. Bootstrap aggregate and random feature extraction are used to average the forest forecasts. RF models have been shown to be reliable predictors for both: small sample numbers and high dimensional data [20]. It is the reason RF is chosen in this study. Figure 7 shows a Random Forest for n classes.

Naïve Bayes (NB) is a probabilistic classifier based on Bayes' theorem, which implies that each feature contributes to the target class independently and equally. It assumes that every feature is independent of the others, which do not interact. Thus, each feature contributes equally to the likelihood of a sample belonging to a certain class. The NB classifier is easy to use and fast to compute. It works well on large datasets with high dimensionality. NB is useful for large applications and is insensitive to noise [21]. These are two reasons for choosing NB in this study. Eq. 2 shows the Naïve Bayes classifier with three features X_1 , X_2 and X_3 .

$$P(y_i|X_1, X_2) = \frac{P(X_1|y_i), P(X_2|y_i), P(y_i)}{P(X_1), P(X_2)} \quad (2)$$

In Eq. 2, two conditional probabilities are calculated for a label if certain features are available based on the conditional property of each feature on the label. The classification label is assigned to the prediction based on the value of the probability.

The hyperparameter used in this study is shown in the Table 3.

This layer applies the bagging algorithm as defined in 1 to the outcomes of all conventional algorithms generated in the classical layer. The notation B_{ci} is used for the representation of the bagging of each considered algorithm. The value of i refers to between 1 and 6 inclusive. Algorithm 1 shows the bagging being applied to individual conventional machine learning algorithms. This layer produces a single outcome, which is based on the performance of the classical layer models and computes the average values of the performance of considered six algorithms.

Table 3 Default parameters for algorithms in scikit-learn

| Algorithm | Default Parameters |
|---------------------------------|---|
| Support Vector Classifier (SVC) | C=1.0, kernel='rbf', degree=3, gamma='scale', coef0=0.0 |
| Logistic Regression (LR) | penalty='l2', C=1.0, solver='lbfgs', max_iter=100 |
| Decision Tree (DT) | criterion='gini', splitter='best', max_depth=None |
| k-Nearest Neighbors (KNN) | n_neighbors=5, algorithm='auto', metric='minkowski' |
| Naive Bayes (NB) | (GaussianNB) var_smoothing=1e-9 |
| Random Forest (RF) | n_estimators=100, criterion='gini', max_depth=None |

Algorithm 1 Bagging Layer Algorithm

```

1: classicalmodels ← [C1, C2, C3, C4, C5, C6]
2: Data ← Dataset
3: ResampledData ← Resampled(Dataset)
4: RLength ← ResampledData.length
5: for model in classicalmodels do
6:   tempmodels ← []
7:   for sample in resampleddata do
8:     tempmodel = models(sample)
9:     tempmodels = tempmodels.add(tempmodel)
10:  end for
11:  Baggingmodel = Bagging(tempmodels)
12: end for

```

This layer accesses all models from the previous layers. First three models from both layers i.e. $C_1, C_2, C_3, B_{C1}, B_{C2}$ and B_{C3} combinely exceed 73% accuracy threshold. Voting is very expensive, therefore, performing all possible combinations can be intensively costly in terms of processing and time. That is the reason the 73% threshold (producing better performance) value is used, which may be changed as per the requirements. The algorithm that takes place at this layer is reported in Algorithm 2. This layer creates a list of subsets for the conventional ML algorithms and bagging method applied in previous both layers at the given threshold value.

The experiments have revealed that not all algorithms exceeded the given threshold of 73%. The voting layer creates separate models for conventional and bagging methods due to processing overhead. The pseudo-code of this layer is presented in 2.

Each layer operates independently on the same input data and feature space. The Classical Layer consists of multiple standalone machine learning algorithms. The Bagging Layer also uses the same feature set but applies bagging ensemble strategies over selected base models. Similarly, the Voting Layer combines outputs from independently trained classifiers using hard or soft voting techniques. These layers signify the selection of algorithms based on performance evaluation on each layer

3.4.2 Evaluation

The evaluation of the proposed approach uses well-established indexes i.e., accuracy, precision, recall, F measure, and ROC (receiver operating characteristic curve), which are described in the following.

The accuracy of a model is shown by the ratio of correctly classified images ($T_P + T_N$) to the total number of images ($T_P + T_N + F_p, F_N$). It is shown in Eq. 3.

$$Accuracy = \frac{T_P + T_N}{T_P + T_N + F_p, F_N} \tag{3}$$

Algorithm 2 Voting Layer Algorithm

```

1: classicalmodels ← [C1, C2, C3, C4, C5, C6]
2: baggingmodels ← [B1, B2, B3, B4, B5, B6]
3: for model in classicalmodels do
4:   if model.accuracy < 75 then
5:     remove model form Classicalmodels
6:   end if
7: end for
8: for model in baggingmodels do
9:   if model.accuracy < 75 then
10:    remove model form baggingmodels
11:   end if
12: end for
13: for models in subset(classicalmodels) do
14:   if models.length ≥ 2 then createvotingclassifier(models)
15:   end if
16:   for models in subset(baggingmodels) do
17:     if models.length ≥ 2 then createvotingclassifier(models)
18:     end if
19:   end for
20: end for

```

The precision of a model is shown by the ratio of correctly predicted images with the drought (T_P) to the total images predicted to have the drought ($T_P + F_P$). It is represented by 4

$$Precision = \frac{T_P}{T_P + F_P} \quad (4)$$

A recall is an evaluation parameter defined by the ratio of correctly predicted drought images (T_P) divided by the total number of images, where there is actually the drought. Mathematically, it is shown by 5

$$Recall = \frac{T_P}{T_P + F_n} \quad (5)$$

F-measure, also known as F-value or F-score, employs both the accuracy and recall scores of a classifier. This metric is widely employed in classification situations. The F-measure is computed by taking the weighted harmonic mean of accuracy and recall. It is represented by 6.

$$F1Score = 2 * \frac{precision * recall}{precision + recall} \quad (6)$$

AUC is a good approach to assess the test's overall diagnostic accuracy. It accepts results ranging [from 0–1]. Zero indicates a totally incorrect test and 1 indicates a fully correct test. The trapezoidal rule may be used to calculate AUC. An AUC of 0.5 indicates no discrimination (i.e., the capacity to classify images with and without the drought), the value 0.7–0.8 is regarded as good, 0.8–0.9 is considered excellent, and greater than 0.9 is considered remarkable.

Table 4 Evaluation parameter scores for classical layer

| Classical layer | | | | | | |
|-----------------|------|--------------|---------|---------|--------|---------|
| Split | Algo | Acc (%) | Pre (%) | Rec (%) | F1 (%) | AUC (%) |
| 80–20 | SVC | 80.83 | 81.54 | 82.81 | 82.17 | 87.08 |
| | LR | 80.83 | 82.54 | 81.25 | 81.89 | 87.47 |
| | RF | 78.33 | 86.54 | 70.31 | 77.59 | 85.41 |
| | DT | 63.33 | 66.67 | 62.50 | 64.52 | 63.39 |
| | KNN | 61.67 | 90.91 | 31.25 | 46.51 | 78.24 |
| | NB | 58.33 | 60.94 | 60.94 | 60.94 | 57.49 |
| 70–30 | SVC | 82.22 | 82.47 | 84.21 | 83.33 | 86.20 |
| | LR | 78.89 | 82.76 | 75.79 | 79.12 | 88.01 |
| | RF | 77.78 | 84.81 | 70.53 | 77.01 | 85.62 |
| | DT | 72.22 | 74.73 | 71.58 | 73.12 | 72.26 |
| | KNN | 58.89 | 80.00 | 29.47 | 43.08 | 74.32 |
| | NB | 59.44 | 61.22 | 63.16 | 62.18 | 58.75 |
| 60–40 | SVC | 80.00 | 82.31 | 81.06 | 81.68 | 85.44 |
| | LR | 82.92 | 86.40 | 81.82 | 84.05 | 88.83 |
| | RF | 74.17 | 85.00 | 64.39 | 73.28 | 83.84 |
| | DT | 69.17 | 73.77 | 68.18 | 70.87 | 69.28 |
| | KNN | 53.33 | 79.41 | 20.45 | 32.53 | 71.85 |
| | NB | 62.08 | 65.19 | 66.67 | 65.92 | 61.33 |

4 Experimental Results

The experiments in this study are performed on Google collab with 16 GB (Gigabytes) RAM (Random Access Memory) and GPU (Graphic Processing Unit) Enabled Runtime. Table 4 shows the results for the classical layer. There are three different splits used i.e., 80–20%, 70–30% and 60–40%. SVM outperformed the classical layer, followed by Logistic Regression and Random Forest. In the 80–20 split, the best performing algorithms are SVM and logistic regression with the accuracy of 80.83%. Logistic regression works really well on binary classification. SVM has the inherent property to perform well on datasets, where the dimensions of the dataset are higher. In 70–30% split, SVM and logistic regression performed better with the accuracy of 82% and 79% respectively. In 60–40% split, SVM and logistic regression with the accuracy of 80% and 82% respectively performed better than other considered algorithms. k-NN and Naive Bayes didn't perform well in comparison with other considered algorithms. k-NN and Naive Bayes throughout each split consistently remained underfitting.

Table 5 shows the results for the bagging layer. In this layer, the performance of a classifier is either equal to the previous layer or its performance is slightly less. The best-performing bagging ensemble is SVM and logistic regression. Bagging is performed on various samples of the training dataset. The performance of the model decreases with a decrease in training data. In 80–20 split, the accuracy of SVM and logistic regression is 81%. In 70–30% split, the accuracy of SVM and logistic regression is 81% and for 60–40% the accuracy is 79% and 80% respectively. The least-performing algorithms are KNN and Naive Bayes. The reason behind the same performance is that bagging creates a model with the same algorithm on a different subset; if the model does not work on the whole set well, then it won't work well for samples as well. Table 5 indicates that classifiers in the bagging layer retain or slightly lower their performance relative to the preceding layer. Reduced training data leads to worse performance, emphasizing the importance of large datasets. KNN and Naive Bayes, on the other hand, are the least successful, most likely because bagging on subsets does not significantly enhance results.

Table 6 shows the experimental results of the voting layer. Table 6 presents the evaluation results for eight combinations of models (M1–M8) in the voting layer. Each model represents a different combination of base

Table 5 Evaluation score for bagging layer

| Bagging layer | | | | | | |
|---------------|------|--------------|---------|---------|--------|---------|
| Split | Algo | Acc (%) | Pre (%) | Rec (%) | F1 (%) | AUC (%) |
| 80–20 | SVC | 80.83 | 83.61 | 79.69 | 81.60 | 87.08 |
| | LR | 80.83 | 85.96 | 76.56 | 80.99 | 87.47 |
| | RF | 77.50 | 84.91 | 70.31 | 76.92 | 85.41 |
| | DT | 72.50 | 81.63 | 62.50 | 70.80 | 63.39 |
| | KNN | 66.67 | 92.86 | 40.63 | 56.52 | 78.24 |
| | NB | 58.33 | 60.94 | 60.94 | 60.94 | 57.49 |
| 70–30 | SVC | 81.11 | 82.11 | 82.11 | 82.11 | 86.20 |
| | LR | 80.56 | 84.88 | 76.84 | 80.66 | 88.01 |
| | RF | 74.44 | 81.01 | 67.37 | 73.56 | 85.62 |
| | DT | 69.44 | 79.41 | 56.84 | 66.26 | 72.26 |
| | KNN | 57.22 | 82.14 | 24.21 | 37.40 | 74.32 |
| | NB | 59.44 | 61.22 | 63.16 | 62.18 | 58.75 |
| 60–40 | SVC | 78.75 | 81.89 | 78.79 | 80.31 | 85.44 |
| | LR | 80.42 | 85.71 | 77.27 | 81.27 | 88.83 |
| | RF | 73.75 | 85.57 | 62.88 | 72.49 | 83.84 |
| | DT | 65.83 | 79.76 | 50.76 | 62.04 | 69.28 |
| | KNN | 48.75 | 69.57 | 12.12 | 20.65 | 71.85 |
| | NB | 65.42 | 69.29 | 66.67 | 67.95 | 61.33 |

classifiers SVC, RF, and LR. Bagging column indicates whether individual or bagging classifiers were used in the voting layer.

As per the model, selection policy on SVM, RF, and LR qualified for this layer. At his layer, the voting method is performed using various subsets of SVM, LR, and RF with both classical and Bagging. The obtained results are significantly worth at this layer. In 80–20% split, voting classifiers containing RF, LR, and SVM provided significant results with a classical approach having accuracy of 84.80%. At 70–30, the highest accuracy score is 84.62% where all three classifiers voted with bagging technique. At 60–40% split, 83.67% remained the highest score with a combination of RF and LR under the bagging scheme. With the decrease in training data, the performance also decreased. The higher performance is achieved with 80–20% split, followed by 70–30% and 60–40%.

Figure 8 reports the timings consumed by the ML algorithms. The highest time is taken by SVM, followed by LR and then DT. The bagging layer takes more time than of the classical layer. Besides, 80–20 split took higher time as compared to 60–40 split. Thus, the training process requires more time in building the model. Interestingly, ML algorithms that produced significantly better outcomes, took more time than that the algorithms, which did not perform well. The time remained directly proportional to the performance of the considered ML algorithms.

ROC-AUC values provide critical insights into the model's discriminative capability across different threshold settings. In our experiments, models, such as SVM and logistic regression, consistently achieved high AUC scores. These results indicate a strong ability to distinguish between drought and no drought classes, even when the decision threshold is varied. A high AUC is especially valuable in drought prediction tasks, where minimizing false positives and false negatives is crucial.

Figure 9 shows the time graph of voting. Each bar represents the time taken by a specific model under a certain split. M1 is a classical model that provides a voting classification for SVM and LR. Looking at Table 6, it is obvious what model corresponds to which combination of classifiers. The highest time is consumed by M5, M6 and M8 because all of them consist of SVM. SVM remained the highest time-consuming model as reported in Fig. 8. These models form a bagging layer, and it can also be seen in Fig. 8. With the decrease in the amount

Table 6 Evaluation results for voting layer

| Voting layer | | | | | | | | |
|--------------|-------|-----|-----|-----|---------|-----------|--------------|---------|
| Split | Model | SVC | RF | LR | Bagging | Classical | F1 Score (%) | AUC (%) |
| 80–20 | M1 | Yes | No | Yes | No | Yes | 81.89 | 57.49 |
| | M2 | Yes | Yes | No | No | Yes | 80.33 | 57.49 |
| | M3 | No | Yes | Yes | No | Yes | 82.54 | 57.49 |
| | M4 | Yes | Yes | Yes | No | Yes | 84.80 | 57.49 |
| | M5 | Yes | No | Yes | Yes | No | 81.97 | 57.49 |
| | M6 | Yes | Yes | No | Yes | No | 80.65 | 57.49 |
| | M7 | No | Yes | Yes | Yes | No | 81.97 | 57.49 |
| | M8 | Yes | Yes | Yes | Yes | No | 81.67 | 57.49 |
| 70–30 | M1 | Yes | No | Yes | No | Yes | 81.32 | 58.75 |
| | M2 | Yes | Yes | No | No | Yes | 81.32 | 58.75 |
| | M3 | No | Yes | Yes | No | Yes | 78.89 | 58.75 |
| | M4 | Yes | Yes | Yes | No | Yes | 81.52 | 58.75 |
| | M5 | Yes | No | Yes | Yes | No | 81.56 | 58.75 |
| | M6 | Yes | Yes | No | Yes | No | 80.22 | 58.75 |
| | M7 | No | Yes | Yes | Yes | No | 80.45 | 58.75 |
| | M8 | Yes | Yes | Yes | Yes | No | 84.62 | 58.75 |
| 60–40 | M1 | Yes | No | Yes | No | Yes | 82.68 | 61.33 |
| | M2 | Yes | Yes | No | No | Yes | 79.03 | 61.33 |
| | M3 | No | Yes | Yes | No | Yes | 82.68 | 61.33 |
| | M4 | Yes | Yes | Yes | No | Yes | 82.68 | 61.33 |
| | M5 | Yes | No | Yes | Yes | No | 82.26 | 61.33 |
| | M6 | Yes | Yes | No | yes | No | 77.55 | 61.33 |
| | M7 | No | Yes | Yes | Yes | No | 83.67 | 61.33 |
| | M8 | Yes | Yes | Yes | Yes | No | 81.30 | 61.33 |

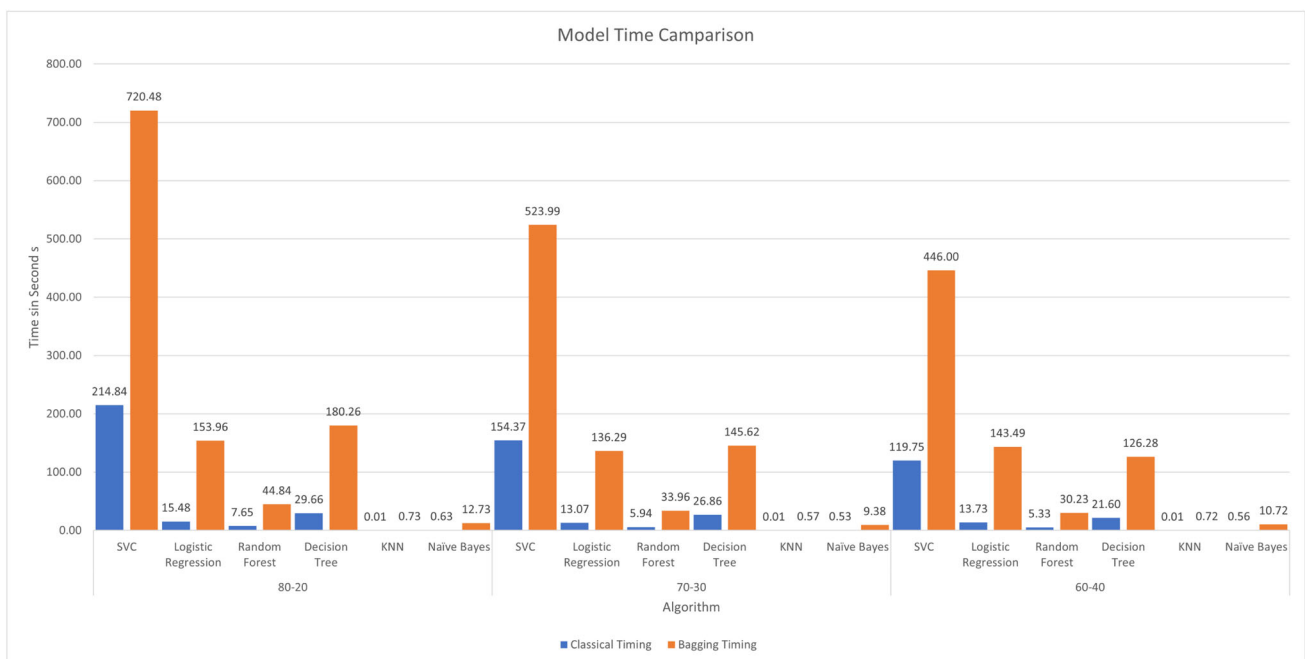


Fig. 8 Models time comparison graph

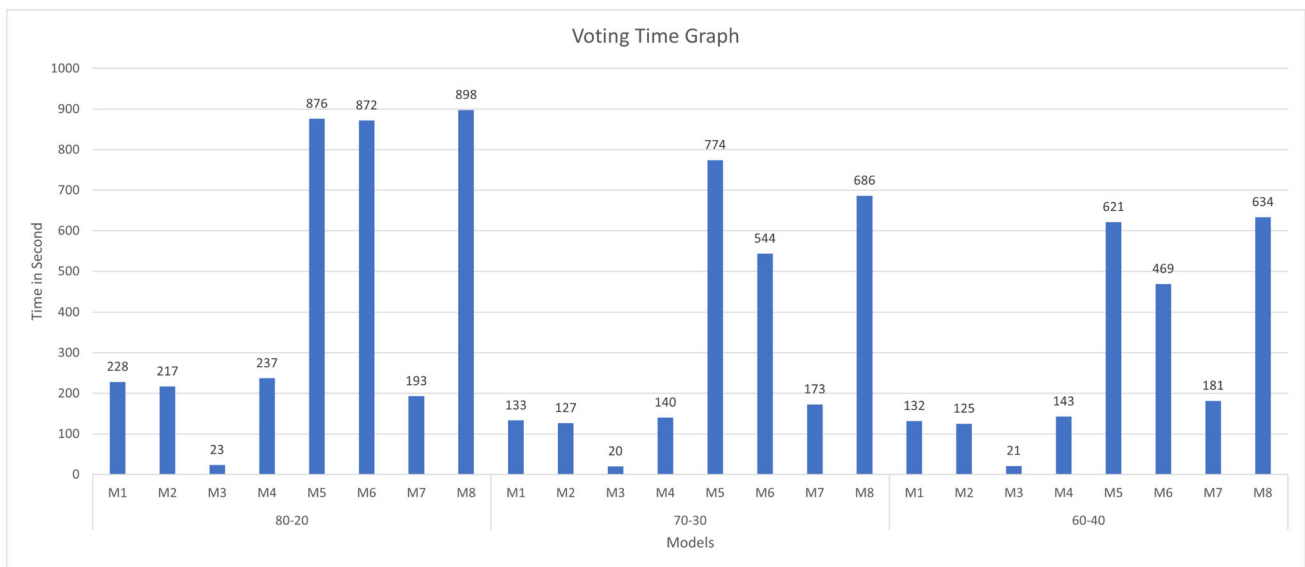


Fig. 9 Models time comparison graph

of training time, time consumption decreases. 60–20% split takes the least training time while 80–20% takes the most time.

5 Conclusions and Future Work

Drought detection using satellite imagery can play an important role in fighting the adverse effects of drought. This study deals with this challenging task with the help of machine learning and image processing. Machine Learning approaches are broadly categorized as classical and ensemble methods. The dataset, used in the experiments, is custom-made using Google earth pro's historical image feature.

This study proposes a layered ensemble approach. There are three layers in the proposed approach: Classical, Bagging, and Voting. In the first layers, the models are trained using classical ML approaches, later these models are used in the bagging layer to create a bagging ensemble of these ML algorithms. In the last layer, models from layer 1 and layer 2 are chosen whose accuracy satisfies a certain threshold. The models, which match the threshold are selected and used in the voting process. The experimental results reported that the SVM and Logistic Regression outperformed other considered algorithms. The bagging ensemble also produced better results using SVM and Logistic Regression. The highest-performing model in terms of accuracy is achieved at layer 3 with an F1 score of 84.80%. The lowest-performing models were Naive Bayes and k-NN. The time consumption of the model is directly proportional to its performance. The models with robust results were taking the highest time and the models with the lowest performance were trained quickly.

Although the proposed approach provided significant results, one of the key limitations of this study is the dataset, which is very limited. The neural networks, other powerful machine learning methods, and deep learning techniques may not be suitable choices for such a limited dataset. Future work would be done by expanding the dataset to apply deep learning models. To enhance the generalization, dataset will be extended by incorporating imagery from alternative satellite sources (e.g., Sentinel, Landsat) and leveraging platforms such as Google Earth Engine, which provide access to broader temporal and spatial datasets.

In the future, it is intended to extend this research work using Convolutional Neural Networks (CNNs) and transfer learning. Additionally, more complicated voting mechanisms, such as TransVoting and Transferensemble, will be applied. This will enable a comparison of the proposed layered architecture with deep learning techniques.

The proposed layered ensemble method can be used in real-time monitoring systems to predict droughts by processing continuous data streams of satellite imagery. It can be deployed on cloud platforms or edge devices. Real-time monitoring system can be used for prompt alerts and decision-making.

Author Contributions Muhammad Owais Raza: Conceptualization, Formal analysis, Funding acquisition, Investigation, Methodology, Validation, Visualization, Writing—original draft, Writing—review & editing. Naeem Ahmed Mahoto: Conceptualization, Formal analysis, Methodology, Project administration, Resources, Software, Validation, Writing—review & editing. Mana Saleh Al Reshan: Conceptualization, Formal analysis, Methodology, Project administration, Validation, Visualization, Writing—review & editing. Ali Alqazzaz: Formal analysis, Methodology, Project administration, Resources, Software, Validation, Writing—review & editing. Adel Rajab: Formal analysis, Methodology, Project administration, Validation, Visualization, Writing—review & editing. Asadullah Shaikh: Formal analysis, Methodology, Project administration, Supervision, Validation, Visualization, Writing—review & editing.

Funding The authors are thankful to the Deanship of Graduate Studies and Scientific Research at University of Bisha for supporting this work through the Fast-Track Research Support Program.

Data Availability The dataset used in this study is not publicly available. However, it can be made available by the corresponding author upon reasonable request.

Declarations

Conflict of interest The authors declare no conflict of interest.

Open Access This article is licensed under a Creative Commons Attribution-NonCommercial-NoDerivatives 4.0 International License, which permits any non-commercial use, sharing, distribution and reproduction in any medium or format, as long as you give appropriate credit to the original author(s) and the source, provide a link to the Creative Commons licence, and indicate if you modified the licensed material. You do not have permission under this licence to share adapted material derived from this article or parts of it. The images or other third party material in this article are included in the article's Creative Commons licence, unless indicated otherwise in a credit line to the material. If material is not included in the article's Creative Commons licence and your intended use is not permitted by statutory regulation or exceeds the permitted use, you will need to obtain permission directly from the copyright holder. To view a copy of this licence, visit <http://creativecommons.org/licenses/by-nc-nd/4.0/>.

References

1. Publisher Trockenheit und dürre im jahr 2018. *BMEL*. (2022,5), <https://www.bmel.de/DE/themen/landwirtschaft/klimaschutz/duerre-2018.html>
2. Felsche, E., Ludwig, R.: Applying machine learning for drought prediction using data from a large ensemble of climate simulations. *Nat. Hazards Earth Syst. Sci. Discuss.* pp. 1–20 (2021)
3. Dikshit, A., Pradhan, B.: Explainable AI in drought forecasting. *Mach. Learn. Appl.* **6**, 100192 (2021)
4. Ullah, A., Khan, D., Zheng, S.: Testing long-run relationship between agricultural gross domestic product and fruits production: evidence from Pakistan. *Ciência Rural*. **48** (2018)
5. Zahraie, B., Nasser, M., Nematizadeh, F.: Exploring spatiotemporal meteorological correlations for basin scale meteorological drought forecasting using data mining methods. *Arab. J. Geosci.* **10**, 1–15 (2017)
6. Sha, S., Wang, L., Hu, D., Ren, Y., Wang, X., Zhang, L.: Agricultural drought model based on machine learning Cubist algorithm and its evaluation. *Hydrology*. **11**, 7 (2024)
7. Xu, X., Chen, F., Wang, B., Harrison, M.T., Chen, Y., Liu, K., Zhang, C., Zhang, M., Zhang, X., Feng, P.: Unleashing the power of machine learning and remote sensing for robust seasonal drought monitoring: A stacking ensemble approach. *J. Hydrol.* **634**, 131102 (2024)
8. Halder, K., Srivastava, A.K., Ghosh, A., Nabik, R., Pan, S., Chatterjee, U., Bisai, D., Pal, S.C., Zeng, W., Ewert, F.: Application of bagging and boosting ensemble machine learning techniques for groundwater potential mapping in a drought-prone agriculture region of eastern India. *Environ. Sci. Eur.* **36**, 155 (2024)
9. Wang, Y., Cui, J., Miao, B., Li, Z., Wang, Y., Jia, C., Liang, C.: Evaluating performance of multiple machine learning models for drought monitoring: A case study of typical grassland in Inner Mongolia. *Land* **13**, 754 (2024)
10. Muraina, I.: Ideal dataset splitting ratios in machine learning algorithms: general concerns for data scientists and data analysts. *Proceedings of the 7th International Mardin Artuklu Scientific Research Conference*, pp. 496–504 (2022)

11. Prasetyo, S., Hartomo, K., Paseleng, M., Candra, D., Simanjuntak, B.: The machine learning to detect drought risk in Central Java using Landsat 8 OLI remote sensing images. In: 2019 5th International Conference On Science And Technology (ICST). **1** pp. 1–6 (2019)
12. Malik, A., Kumar, A.: Meteorological drought prediction using heuristic approaches based on effective drought index: a case study in Uttarakhand. *Arab. J. Geosci.* **13**, 1–17 (2020)
13. Shahbazi, A., Zahraie, B., Sedghi, H., Manshouri, M., Nasser, M., et al.: Seasonal meteorological drought prediction using support vector machine. *World Appl. Sci. J.* **13**, 1387–1397 (2011)
14. Belayneh, A., Adamowski, J., Khalil, B., Quilty, J.: Coupling machine learning methods with wavelet transforms and the bootstrap and boosting ensemble approaches for drought prediction. *Atmos. Res.* **172**, 37–47 (2016)
15. Park, S., Im, J., Park, S., Rhee, J.: Drought monitoring using high resolution soil moisture through multi-sensor satellite data fusion over the Korean peninsula. *Agric. Forest Meteorol.* **237**, 257–269 (2017)
16. Raza, O., Memon, M., Bhatti, S., Pathan, N.: Drought prediction with raw satellite imagery and ensemble supervised machine learning. *Rev. Environ. Earth Sci.* **8**, 1–7 (2021)
17. Roy, K., Kar, S., Das, R.: Understanding the basics of QSAR for applications in pharmaceutical sciences and risk assessment. Academic Press (2015)
18. Sinnott, R., Duan, H., Sun, Y.: Chapter 15-a case study in big data analytics: exploring twitter sentiment analysis and the weather. *Big Data*. pp. 357–388 (2016)
19. Matzavela, V., Alepis, E.: Decision tree learning through a predictive model for student academic performance in intelligent m-learning environments. *Comput. Educ. Artific. Intell.* **2**, 100035 (2021)
20. Williams, B., Cremaschi, S.: Selection of surrogate modeling techniques for surface approximation and surrogate-based optimization. *Chem. Eng. Res. Design.* **170**, 76–89 (2021)
21. Li, H.: Machine learning for the subsurface characterization at core, well, and reservoir scales. (2020)
22. Abar, T., Letaifa, A., El Asmi, S.: User behavior-ensemble learning based improving QoE fairness in HTTP adaptive streaming over SDN approach. *Adv. Comput.* **123**, 245–269 (2021)
23. Feng, P., Wang, B., Li Liu, D., Yu, Q.: Machine learning-based integration of remotely-sensed drought factors can improve the estimation of agricultural drought in South-Eastern Australia. *Agric. Syst.* **173**, 303–316 (2019)
24. Tan, R., Perkowski, M.: Wavelet-Coupled machine learning methods for drought forecast utilizing hybrid meteorological and remotely-sensed data. In: Proceedings of the International Conference on Data Mining (DMIN'15). (2015)
25. Jalili, M., Gharibshah, J., Ghavami, S., Beheshtifar, M., Farshi, R.: Nationwide prediction of drought conditions in Iran based on remote sensing data. *IEEE Trans. Comput.* **63**, 90–101 (2013)
26. Proadhan, F., Zhang, J., Yao, F., Shi, L., Pangali Sharma, T., Zhang, D., Cao, D., Zheng, M., Ahmed, N., Mohana, H.: Deep learning for monitoring agricultural drought in south Asia using remote sensing data. *Remote Sensing.* **13**, 1715 (2021)
27. Khan, N., Sachindra, D., Shahid, S., Ahmed, K., Shiru, M., Nawaz, N.: Prediction of droughts over Pakistan using machine learning algorithms. *Adv. Water Resour.* **139**, 103562 (2020)
28. Das, P., Naganna, S., Deka, P., Pushparaj, J.: Hybrid wavelet packet machine learning approaches for drought modeling. *Environ. Earth Sci.* **79**, 1–18 (2020)
29. Saha, S., Gayen, A., Gogoi, P., Kundu, B., Paul, G., Pradhan, B.: Proposing novel ensemble approach of particle swarm optimized and machine learning algorithms for drought vulnerability mapping in Jharkhand, India. *Geocarto Int.* pp. 1–32 (2021)
30. Neeti, N., Murali, C., Chowdary, V., Rao, N., Kesarwani, M.: Integrated meteorological drought monitoring framework using multi-sensor and multi-temporal earth observation datasets and machine learning algorithms: A case study of central India. *J. Hydrol.* **601**, 126638 (2021)
31. Ganguli, P., Reddy, M.: Ensemble prediction of regional droughts using climate inputs and the SVM–copula approach. *Hydrol. Process.* **28**, 4989–5009 (2014)
32. Nay, J., Burchfield, E., Gilligan, J.: A machine-learning approach to forecasting remotely sensed vegetation health. *Int. J. Remote Sens.* **39**, 1800–1816 (2018)
33. Elbeltagi, A., Kumari, N., Dharpure, J., Mokhtar, A., Alsafadi, K., Kumar, M., Mehdinejadani, B., Ramezani Etedali, H., Brouziyne, Y., Towfiqul Islam, A., et al.: Prediction of combined terrestrial evapotranspiration index (CTEI) over large river basin based on machine learning approaches. *Water* **13**, 547 (2021)
34. Proadhan, F., Zhang, J., Sharma, T., Nanzad, L., Zhang, D., Seka, A., Ahmed, N., Hasan, S., Hoque, M., Mohana, H.: Projection of future drought and its impact on simulated crop yield over South Asia using ensemble machine learning approach. *Sci. Total Environ.* **807**, 151029 (2022)
35. Morid, S., Smakhtin, V., Bagherzadeh, K.: Drought forecasting using artificial neural networks and time series of drought indices. *Int. J. Climatol. A J. R. Meteorol. Soc.* **27**, 2103–2111 (2007)
36. Jiang, X., Chen, S.: Application of weighted Markov SCGM (1, 1) C model to predict drought crop area. *Syst. Eng. Theory Practice.* **29**, 179–185 (2009)
37. Sundararajan, K., Garg, L., Srinivasan, K., Bashir, A., Kaliappan, J., Ganapathy, G., Selvaraj, S., Meena, T.: A contemporary review on drought modeling using machine learning approaches. *CMES-Comput. Model. Eng. Sci.* **128**, 447–487 (2021)

38. Agana, N., Homaifar, A.: A deep learning based approach for long-term drought prediction. *SoutheastCon* **2017**, 1–8 (2017)
39. Shen, R., Huang, A., Li, B., Guo, J.: Construction of a drought monitoring model using deep learning based on multi-source remote sensing data. *Int. J. Appl. Earth Observ. Geoinform.* **79**, 48–57 (2019)
40. Docheshmeh Gorgij, A., Alizamir, M., Kisi, O., Elshafie, A.: Drought modelling by standard precipitation index (SPI) in a semi-arid climate using deep learning method: long short-term memory. *Neural Comput. Appl.* **34**, 2425–2442 (2022)
41. Mishra, A., Desai, V., Singh, V.: Drought forecasting using a hybrid stochastic and neural network model. *J. Hydrol. Eng.* **12**, 626–638 (2007)
42. Bacanli, U., Firat, M., Dikbas, F.: Adaptive neuro-fuzzy inference system for drought forecasting. *Stoch. Environ. Res. Risk Assessm.* **23**, 1143–1154 (2009)
43. Dastorani, M., Afkhami, H., Sharifidarani, H., Dastorani, M., et al.: Application of ANN and ANFIS models on dryland precipitation prediction (case study: Yazd in central Iran). *J. Appl. Sci.* **10**, 2387–2394 (2010)
44. Kelishadrokh, M.K., Ghattaei, M., Fekri-Ershad, S.: Innovative local texture descriptor in joint of human-based color features for content-based image retrieval. *Signal Image Video Process* **17**(8), 4009–4017 (2023)
45. Iqra A, Mahboob MA. Spatio-temporal mapping of Tharparkar drought using high resolution satellite remote sensing data. *Sci. Int.* **281** (2016)

Publisher's Note Springer Nature remains neutral with regard to jurisdictional claims in published maps and institutional affiliations.

Authors and Affiliations

Muhammad Owais Raza¹ · Naeem Ahmed Mahoto² · Mana Saleh Al Reshan^{3,4} · Ali Alqazzaz⁵ · Adel Rajab⁶ · Asadullah Shaikh^{3,4}

✉ Asadullah Shaikh
asshaikh@nu.edu.sa

Muhammad Owais Raza
6210024002@std.izu.edu.tr

Naeem Ahmed Mahoto
naeem.mahoto@faculty.muett.edu.pk

Mana Saleh Al Reshan
msalreshan@nu.edu.sa

Ali Alqazzaz
aqzaz@ub.edu.sa

Adel Rajab
adrajab@nu.edu.sa

¹ Department of Computer Engineering, Istanbul Sabahattin Zaim University, Istanbul 34303, Turkey

² Department of Software Engineering, Mehran University of Engineering and Technology, Jamshoro 76062, Sindh, Pakistan

³ Department of Information Systems, College of Computer Science and Information Systems, University of Najran, Najran 61441, Saudi Arabia

⁴ Emerging Technologies Research Lab (ETRL), College of Computer Science and Information Systems, University of Najran, Najran 61441, Saudi Arabia

⁵ College of Computing and Information Technology, University of Bisha, Bisha 61922, Saudi Arabia

⁶ Department of Computer Science, College of Computer Science and Information Systems, University of Najran, Najran 61441, Saudi Arabia